Solid Earth Discuss., doi:10.5194/se-2016-89, 2016
Manuscript under review for journal Solid Earth
Published: 30 June 2016

Solid Earth Discussions
Open Access
EGU

Ionospheric influence on the seismo-telluric current related to electromagnetic signals observed before the Wenchuan M_S=8.0 earthquake

Mei Li[1, 2], Handong Tan[2] and Meng Cao[2]

(1) China Earthquake Networks Center, China Earthquake Administration, No.5, Sanlihe Nanhengjie, Xicheng District, 100045 Beijing, China.
(2) China University of Geosciences, No.29, Xueyuan Road, Haidian District, 100083 Beijing, China.

Corresponding author: Handong Tan, China University of Geosciences, No.29, Xueyuan Road, Haidian District, 100083 Beijing, China. (thd@cugb.edu.cn)

Abstract. A three-layer (Earth-air-ionosphere) physical model, as well as a two-layer (Earth-air) model, is employed in this paper to investigate the ionospheric effect on the wave fields for a finite length dipole current source co-located with the main fault of an earthquake when the transmitter-receiver distance is up to one thousand kilometers or even more. The results show that all electrical fields are free of the ionospheric effect for different frequencies in a relative short range, e.g., ～300 km for f=1 Hz, implying the ionospheric influence on electromagnetic fields can be neglected within this range that becomes smaller as the frequency increases. However, the ionosphere can give a constructive interference to the waves passed through and make them decay slowly when an observation is out of this range and the ionosperic effect can be up to 1-2 magnitudes of the electrical fields. For an observed 1.3 mV/m signal at 1,440 km away for the Wenchuan M_S=8.0 earthquake, the expected seismo-telluric current magnitude for the Earth-air-ionosphere model is of 5.0×10^4 kA , which is of one magnitude smaller than the current value of 3.7×10^5 kA obtained by the Earth-air model free of ionospheric effect. This indicates that the ionosphere facilitates the electromagnetic wave propagation, as if the detectability of the system is improved effectively and it is easier to record a signal even for stations located at distances beyond their detectability threshold.

Keywords. Ionospheric influence on electromagnetic waves; The Wenchuan earthquake; Seismo-telluric current

Solid Earth Discuss., doi:10.5194/se-2016-89, 2016
Manuscript under review for journal Solid Earth
Published: 30 June 2016

1 Introduction

The fact that Electro-Magnetic (EM) emissions accompany every stage of large earthquake preparations seems undebatable although short-term earthquake prediction is still one of the most challenging targets in Earth science today (Eftaxias et al., (2002). Meanwhile, the Ultra-Low Frequency (ULF) band is of particular interest because only EM signals in the ULF range and at lower frequencies originated in the Earth's crust can be easily recorded at the Earth's surface without significant attenuation comparing with 'high' frequency emissions that might be emitted at epicenter depths at more than 10 km, even several hundreds of kilometers. Recently, ULF electromagnetic anomalous phenomena related to strong earthquakes have been investigated and reported in increasing numbers. Two notable examples are the Loma Prieta *M*s=7.1 earthquake on October 17, 1989 (Fraser-Smith et al., 1990; Bernardi et al., 1991), as well as the Spitak M_S=6.9 earthquake on December 7, 1988 [Molchanov et al., 1992; Kopytenko et al., 1993). It was found that, these two earthquakes have very similar electromagnetic emission fluctuation characteristics. The intensity of the signals began to increase 3-5 days before the earthquake at Spitak and 12 days before that at Loma Prieta. The most important point is the electromagnetic emissions exhibited a maximum 4 h before the Spitak event (f=0.005-1 Hz, D=200 km, A=0.2 nT) and 3 h before the Loma Prieta event (f=0.01-10 Hz, D=7 km, A=1.5 nT).

A more recent example reported by Li et al. (2013) is the Wenchuan *M*s=8.0 earthquake on May 12, 2008, a typical mid-crust, which resulted in great devastation and 69,000 deaths. This earthquake was preceded by more than one month of increasing anomalous ULF emissions with a climax starting on May 9, three days before the Wenchuan main shock (f=0.1-10 Hz, D=1,440 km, A=1.3 mV m-1).

Many simulating rock-pressure experiments were carried out in order to understand the producing mechanism of the electromagnetic information associated with seismic activities. Laboratory experiments by Qian et al., (1996; 2003) and Hao et al. (2003) demonstrate that, electromagnetic signals are always recorded when rock samples are subjected to dynamic stresses. There is a close relationship between the produced signal and the formation of micro-cracks in the rock. Furthermore, the climax of the signal occurred when the main rupture happened and the magnetic pulses of shorter-period appearing at the last stage of the experiment may be induced by instantaneous electric current of the accumulated charge during the cracking acceleration. Strong electromagnetic signals are generated while rock samples were

Solid Earth Discuss., doi:10.5194/se-2016-89, 2016
Manuscript under review for journal Solid Earth
Published: 30 June 2016

fracturing (Panfilov, 2014). As rocks upon stressing, dislocations are generated that sweep through the mineral grains and break the peroxy links. The positive holes are activated as charge carriers, and have the remarkable capability to flow out of the stressed sub-volume and spread into the surrounding unstressed rocks. This situation can be considered as analogous to a battery which generates electric currents along the stress-gradient direction (Freund, 2002; Freund and Sornette, 2007; Freund, 2009, 2010). A gabbro sample（30×15×10 cm^3）from Shanxi, China, came into the test and a 55 nA current recorded about 2 seconds before failure, with the load being at about 30,000 lbs and the maximum spike reaches 450 nA when the main failure took place (Freund, 2009). Up to now, no clear explanation has been given although several physical mechanisms have been proposed to interpret the generation of EM emissions and electrical currents observed either during seismic activity or in the laboratory experiments. These include the electrokinetic and magnetohydrodynamic, piezomagnetism, stress-induced variations in crustal conductivity, microfracturing, and so on (Draganov et al., 1991; Park, 1996; Fenoglio et al., 1995; Egbert, 2002; Simpson and Taflove, 2005). Whatever the physical mechanism of electromagnetic generation is, it is well established that, during rock experiments conducted under laboratory conditions, a strong electrical current is produced when rocks are stressed, especially at the stage of the main rupture. So, like what Bortnik et al. (2010) wanted to know, what is the electrical current necessary to produce an observable magnetic signal on the ground, at a given distance from the epicenter and for an assumed ground conductivity? In their work, an infinitesimally short, horizontal dipole located at a hypocenter depth in the half-space (Earth) is used to estimate the magnitude of the seismo-telluric current required for the “Alum Rock” M_W=5.6 earthquake on October 31, 2007. The observable electromagnetic ground signals (f=1 Hz, D=2 km, A=30 nT) and the results show that for an observed 30 nT pulse at 1 Hz, the expected seismo-telluric current magnitudes fall in the range ~10–100 kA.

Unlike a parameter of the “Alum Rock” M_W=5.6 earthquake (D=2 km), the distance between the epicenter of the Wenchuan M_S=8.0 earthquake and the observing station is D~1,440 km (Li et al., 2013), i.e. several times higher than the height of the bottom of ionosphere (h~85-100 km) (Kuo et al., 2011; Cummer, 2000; Yamauchi et al., 2007). When we investigate electromagnetic emissions induced by an electrical current or a magnetic moment on the surface or beneath the Earth, the effect of the medium air, crustal as well as ionosphere should be taken into account because of

Solid Earth Discuss., doi:10.5194/se-2016-89, 2016
Manuscript under review for journal Solid Earth
Published: 30 June 2016

these three media being of different conductivities and so we need to consider a lithosphere-atmosphere-ionosphere electromagnetic coupling. The ionosphere plays an important role in radio propagation at Extremely Low Frequency (ELF) and Very Low Frequency (VLF), the ground and the ionosphere are good electrical conductors and form a spherical Earth-ionosphere waveguide (Cummer, 2000). In addition, in the magneto-telluric (MT) method, widely used in exploring petroleum or mine, the ionospheric influence on electromagnetic (EM) fields should be considered when the transmitter-receiver distance of a large-scale and large-power fixed resource is up to one thousand kilometers. EM fields can be strengthened in the ionosphere as it is shown when we use analytical solutions of Maxwell equations, as well as numerical ones of the "Earth-ionosphere" mode with a source on the ground or in the air (Fu et al., 2012; Li et al., 2010a; Li et al., 2010b; Xu et al., 2012; Li et al., 2011). Therefore, comparing with an electromagnetic attenuation without ionospheric effect, the point is to evaluate the ionospheric influence on the electromagnetic propagation when the transmitter-receiver distance is up to one thousand kilometers or even more. Furthermore, the comparison between the observation distance (D=1,440 km) and the length of the Wenchuan earthquake main rupture L=～150 km (Zhang et al., 2009) indicates that the length of the dipole source is not negligible. So in this paper, using the work of Key (2009), a three-layer (Earth-air-ionosphere) physical model, as well as a two-layer (Earth-air) model, containing a finite length dipole current source co-located along the fault and beneath the Earth is introduced in Sect. 2. For specified parameters, some simulation results of the dipole source with and without ionospheric effect are given in Sect. 3. In Sect.4, we define and limit our assumed parameter values, present the results for the Wenchuan earthquake case. Discussion and conclusions are given in Sect. 5 and Sect.6, respectively.

2 Description of the modeling methodology

In order to study the electromagnetic fields emitted by a long dipole current source, the approach used here follows the magnetic vector potential formulation described in Wait (1982) and developed by Key (2009), who generalized the formulation to allow for multiple layers above the transmitter (in addition to multiple layers below). He used exponential forms for the recursions rather than hyperbolic functions in isotropic media, which consists of N layers of isotropic conductivityσ_i where$i = 1, \ldots, N$, and which uses a right-handed coordinate system with the z axis

Solid Earth Discuss., doi:10.5194/se-2016-89, 2016
Manuscript under review for journal Solid Earth
Published: 30 June 2016

pointing down. Assuming a time-harmonic source with $e^{-i\omega t}$ time dependence, negligible magnetic permeability μ variations, and angular frequencies ω that are low enough so that displacement currents can be neglected, Maxwell's equations are

$$\nabla \times \mathbf{E} = i\omega\mathbf{B}, \quad (1)$$

and

$$\nabla \times \mathbf{B} = \mu\sigma\mathbf{E} + \mu\mathbf{J}_s . \quad (2)$$

Expression $\mathbf{J}_s = \mathbf{I}\delta(\mathbf{r} - \mathbf{r_0})$ is the imposed electric dipole source at position $\mathbf{r}_0$ with vector moment **I**, and here is restricted to an infinitesimal dipole with unit moment.

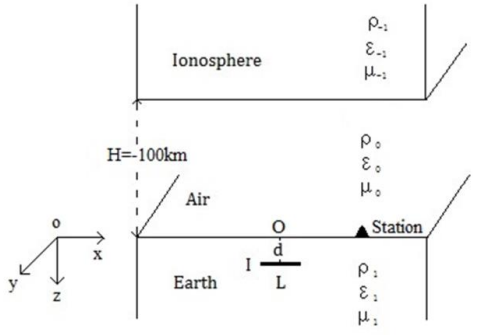

Fig.1. An x-directed dipole current source, with its central coordinate (0, 0, d), is placed in the bottom medium (Earth) of a three layer modeling (Earth-air-ionosphere model), where z is defined positive in the downward direction.

Based on the model set up by Key (2009), some modifications will be done in this study in order to answer the questions illustrated above. A physical model is specified. It has three layers, Earth, air and ionosphere, which is called Earth-air-ionosphere model. Its coordinate system is denoted in Fig.1 with z-direction being downward. An x-directed dipole of a length L and a current I is placed in the bottom medium (Earth: $z > 0$), which is homogeneous and has the electrical properties: magnetic permeability μ_1, permittivity ε_1, and conductivity σ_1. The middle medium (air: $-100\ \text{km} < z < 0$) is described by its electrical properties μ_0, $\varepsilon_0 (= 8.854 \times 10^{-12}\ \text{Farad m}^{-1})$ and $\sigma_0 (= 10^{-14}\ \text{S m}^{-1})$. The top medium (ionosphere: $z < -100\ \text{km}$) is characterized by electrical properties μ_{-1}, ε_{-1} and $\sigma_{-1} (= 10^{-5}\ \text{S m}^{-1})$.

Solid Earth Discuss., doi:10.5194/se-2016-89, 2016
Manuscript under review for journal Solid Earth
Published: 30 June 2016

As a comparison, a two-layer model (Earth-air model) including in Earth medium ($z > 0$), as well as air medium ($z < 0$), is also established during the study. All the corresponding parameters described are the same as these of Earth-air-ionosphere model.

We assume that the total space is non-magnetic and that the magnetic permeabilityμvariations are negligible in the different layers, i.e. $\mu_1 = \mu_0 = \mu_{-1} = 4\pi \times 10^{-7}$ Farad m^{-1}. However, the ionosphere as the electrically conducting section of the upper atmosphere play a so important role on the electromagnetic propagation that we set $\varepsilon_{-1} = 5\varepsilon_0$ when an ionospheric effect on electromagnetic transmission is taken into consideration. On the same manner we have $\varepsilon_1 = \varepsilon_0 = 8.854 \times 10^{-12}$ Farad m^{-1}, i.e. ε_1 is not considered as zero during all calculations. Under these conditions, the formula listed above are still suitable and more explanations about the potential formulation of a horizontal electric dipole can be found in the Appendix A of Key (2009) and related programs are available with an access to the website (http://marineemlab.ucsd.edu/). The horizontal finite length dipole source can be seen as an integral of an infinite small horizontal dipole during related calculations.

3 Simulation results

According to these two models built above, several free parameters must be specified in order to investigate the attenuation characteristics of the electromagnetic fields emitted by a long x-directed dipole current source. As for the parameters of the dipole current source, we select L=150 km, the Wenchuan earthquake main rupture stage within 30 s out of 90 s (~300 km) based on Zhang et al., (2009, Fig.1), the depth d =19 km (Xu, 2009), the hypocenter depth of the Wenchuan case and the current is set to be I=1 A temporarily. Here, the Earth is considered to be an isotropic media with an average conductivity σ_1, and we assume $\sigma_1 = 1.0 \times 10^{-3}$ S m^{-1} at this time, i.e. $\rho_1 = 10^3$ ohm · m, although the ground conductivity depends not only on the local petrology, but also on the porosity, temperature, and pressure (e.g., Wait, 1966). All these parameters are common to two models. While the parameter $\varepsilon_{-1} = 5\varepsilon_0$ is of most importance during the calculation in three-layer model in that it potentially can affect the transmission of electromagnetic waves produced by the dipole beneath the Earth, and possibly induces the Earth-atmosphere-ionosphere electromagnetic coupling.

Solid Earth Discuss., doi:10.5194/se-2016-89, 2016
Manuscript under review for journal Solid Earth
Published: 30 June 2016

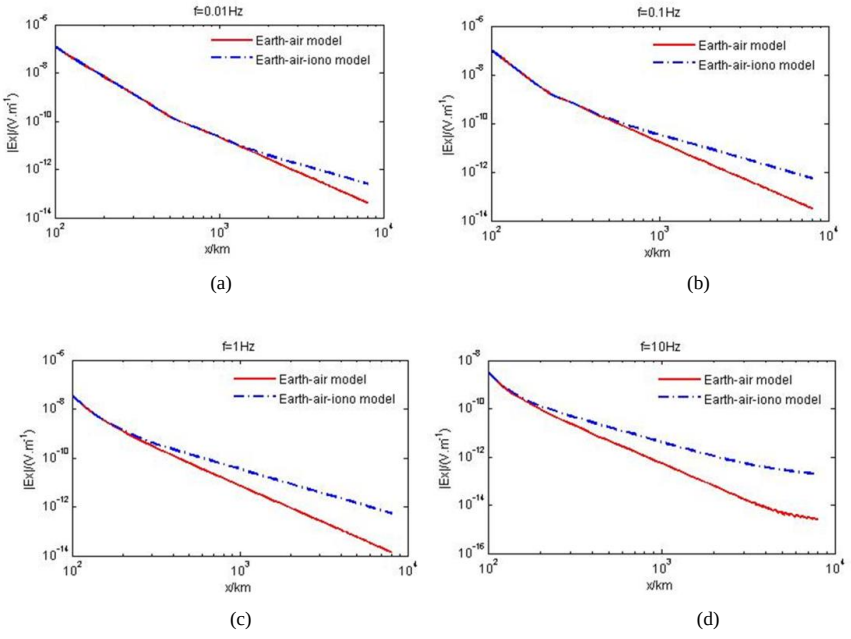

Fig.2. Electric field $|E_x|$ decay curves along x-axial direction as a function of the observing distance for the Cartesian coordinate system with different frequencies. Red solid lines stand for electric field curves for Earth-air model and blue dot lines denote electric field curves with the ionospheric effect for Earth-air-ionosphere model.

(a) Total $|E_x|$ for f=0.01 Hz; (b) Total $|E_x|$ for f=0.1 Hz;
(c) Total $|E_x|$ for f=1 Hz; (d) Total $|E_x|$ for f=10 Hz;

Fig.2a-d displays electric field component amplitude $|E_x|$ decay curves along the x-axial direction with the frequencies f=0.01 Hz, f=0.1 Hz, f=1 Hz, and f=10 Hz respectively for the Cartesian coordinate system up to ~10,000 km on the Earth's surface.

It can be seen from Fig.2a-d, first, the electrical field with "high" frequency has a big attenuation although all curves for both Earth-air model (red solid lines) and Earth-air-ionosphere model (blue dot lines) decay rapidly as the distance increases. Second, each group of curves run at the same level for one fixed frequency, e.g., f=1 Hz, when an observing point is located at a relative near distance, ~300 km for f=1 Hz (Fig.2c) for example. That is to say, the ionospheric influence on electromagnetic field transmissions can be neglected within this range. However this range changes

Solid Earth Discuss., doi:10.5194/se-2016-89, 2016
Manuscript under review for journal Solid Earth
Published: 30 June 2016

for different frequencies and it becomes smaller as the operating frequency of the current source increases (e.g., more than 1000 km for f=0.01 Hz (Fig.2a) and only ~200 km for f=10 Hz (Fig.2d)). Third, the most important result is, as the distance increases, field curves with an ionospheric effect (blue dot lines) run by a different way from that of curves without an ionospheric effect (red solid lines) and the ionospheric lines attenuate more slowly. Now, this kind of ionospheric influence cannot be neglected at this time anymore. The ionospheric difference is about 1 magnitude (×10) for all the frequencies listed and even once up to 2 magnitudes for f=10 Hz within the range shown in Fig.2. For example, the ionospheric difference value shows 1 magnitude from ～840 km, up to 2 magnitudes from ～3,700 km for f=10 Hz (Fig.2d).

4 The Wenchuan M_S=8.0 earthquake as a sample

4.1 Estimating the seismo-telluric current magnitude

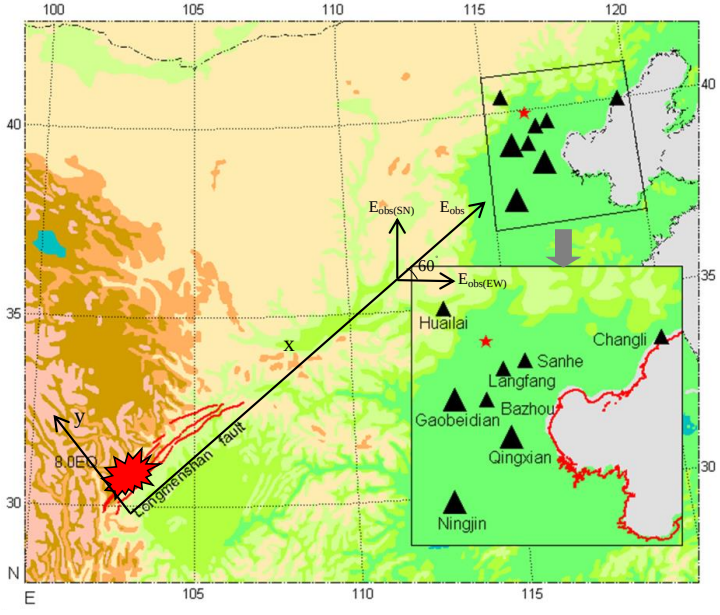

Fig.3. Distribution of the Wenchuan earthquake epicenter and observation stations. Black solid triangles present the related locations of observation stations in Hebei electromagnetic observation network, bigger ones indicate the stations where abnormal information was recorded and the red star denotes Beijing (Li et al., 2013, Fig.1). A ground surface coordinate system is added.

Solid Earth Discuss., doi:10.5194/se-2016-89, 2016
Manuscript under review for journal Solid Earth
Published: 30 June 2016

On the base of the work of rock experiments conducted under laboratory conditions, there is a reason to believe that a giant seismo-telluric current is generated when the main rupture took place during the Wenchuan earthquake on 12 May 2008 and that this current mainly propagates along the Longmenshan fault. At the same time a strong electrical field induced by this current suddenly increased. This electrical field was recorded at the ground-based Gaobeidian observing station, 1440 km away from the epicenter of the shock, with a SN maximum amplitude of 70 mm, i.e. 1.3 mV m^{-1} (Li et al., 2013), that is $E_{obs(SN)}$ = 1.3 mV m^{-1} in the following statement (Fig. 3).

In order to establish a relationship between the seismo-telluric current during the main event and the observable ground electrical signals registered at Gaobeidian station, we consider that a finite length current dipole source, with the length being the main rupture L=150 km of the Wenchuan earthquake and the current I, is co-located with the Longmenshan main fault (x-direction), with the depth being d=19 km. Then one can refer to Fig.1 with ionospheric effect.

A coordinate system on the Earth's surface (see Fig.3) is set up to calculate the observable electrical field along the x-direction E_{obs} according to the electrical value $E_{obs(SN)}$=1.3 mV m^{-1} recorded at the Gaobeidian station. The Gaobeidian station lies in the extended line of the Longmenshan fault, which trends northeast and dips about 60 °west (Xu, 2009). Other locations of stations are shown in Fig.1 of Li et al. (2013) and here they are shown in Fig.3 which includes a ground surface coordinate system. From Fig.3, we see that the electrical filed component intensity along the x-direction is about $|E_x|$=E_{obs}=1.5 mV m^{-1} ($E_{obs(SN)}$=sin60 °×E_{obs}=1.3 mV m^{-1} → E_{obs}=1.5 mV m^{-1}).

As the observing frequency of the electromagnetic observation system is 0.1-10 Hz and the recorder belongs to a real-time analog record, it is not easy to finger out the right frequency of the signals registered at the Gaobeidian station during the maximum stage prior to the Wenchuan earthquake. We set the main frequency f=1 Hz during our calculations although the information is of a short period ~0.1-0.3 s and a large amplitude ~1.3 mV m^{-1} (Li et al., 2013) and frequency bands (0.4-3 s and 0.05-0.1 s) with various amplitudes were observed (Guan et al., 2003). At the same time, the results of 2D MT inversion in the Longmenshan fault show that the apparent resistivity logarithm is ～1-4.8 (Zhu et al., 2008) and it is a wide range.

Solid Earth Discuss., doi:10.5194/se-2016-89, 2016
Manuscript under review for journal Solid Earth
Published: 30 June 2016

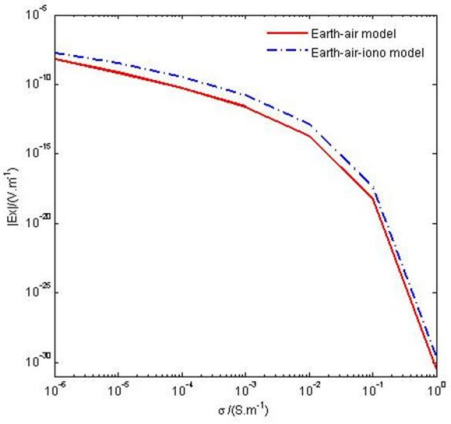

Fig.4. The calculated value of |Ex|, expected at the observation location (1,440 km, 0, 0) due to a dipole source of L=150 km, I=1 A, f=1 Hz and d=19 km (Fig.1), as a function of the typical crustal materials conductivity σ both in Earth-air model (red line) and in Earth-air-ionosphere model (blue dot line).

Fig. 4 shows the calculated values of |Ex|, expected at the observation location (1,440 km, 0, 0) due to a dipole source of L=150 km, I=1 A and d=19 km (Fig.1), as a function of the typical crustal materials conductivity σ. Comparing with the red line with the blue dot one, the ionospheric effect is clearly displayed throughout the variation of the crustal conductivity. A rapid attenuation (exceed 20 orders) of the field values indicates the importance of the conductivity σ. It is difficult to specify the average conductivity σ (referred to as σ_1 in the context) of the homogeneous Earth medium, even for the typical Wenchuan area. However, combined with f=1 Hz here, the skin-depth depends on the conductivity σ, given by the formula $\delta = (\pi f \mu_0 \sigma)^{-\frac{1}{2}}$. Taken the depth d=19 km into account, here $\delta = d = 19$ km and the calculated σ_1 is attained, i.e. $\sigma_1 = 7.0 \times 10^{-4}$ S m^{-1}, which is advantageous to radiate electromagnetic waves within this depth.

Using the same parameters as above, the simulation results show that the seismo-telluric current along the main fault needed to produce an electrical ground signal $E_{obs(SN)}$ = 1.3 mV m^{-1} at the Gaobeidian station when the Wenchuan event occurred, is about 5.3×10^4 kA with the ionospheric effect and 3.7×10^5 kA without the ionospheric effect. As it is expected, these two results have one order ($\times 10$)

Solid Earth Discuss., doi:10.5194/se-2016-89, 2016
Manuscript under review for journal Solid Earth
Published: 30 June 2016

difference from each other. While the former is more reasonable under this conditions because the seismo-telluric current produced by the Wenchuan main rupture is specified.

4.2. Detectability under the ionospheric effect

Now according to the Wenchuan earthquake example, the seismo-telluric current source (f=1 Hz, d =19 km, L=150 km, and a current I=5.3×10^4 kA considering the Earth-air-ionosphere model) is thought of as a powerful finite length dipole source.

Fig.5 displays the fluctuations of the surface electrical fields with and without ionospheric effect for the Wenchuan source along x-axial direction. It shows no obvious ionospheric effect within 300 km, while this effect is roughly up to 1 magnitude from ~800 km. The gap becomes larger as the distance extends, 2 magnitudes from ~4000 km, and then it keeps this gap till 10,000 km. Under this condition, considering the observable signal 1.5 mV m^{-1} at Gaobeidian station before the Wenchuan epicenter, the distance recorded such a signal must be ～1500 km (blue arrow) with ionospheric effect, or it is only ～800 km (red arrow) without ionospheric effect. So the ionosphere facilitates the electromagnetic wave propagation, as if the detectability of the system is improved effectively and it is easier to record a signal even for stations located at distances beyond their detectability threshold.

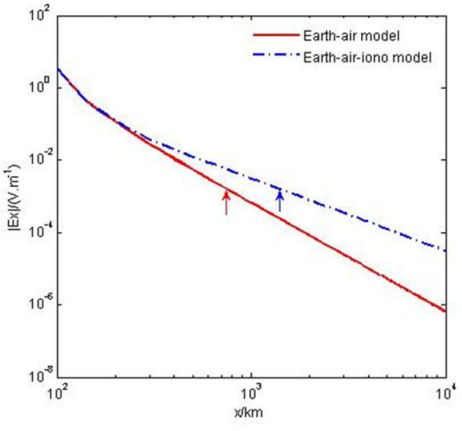

Fig.5. The Wenchuan source producing electric field |Ex| decay curves as a function of the distance along x-axial direction with ionospheric effect (blue dot line), as well as without ionospheric effect (red line). The electric field |Ex|=1.5 mV m^{-1} is labeled by a red arrow and a blue one respectively.

Solid Earth Discuss., doi:10.5194/se-2016-89, 2016
Manuscript under review for journal Solid Earth
Published: 30 June 2016

5 Discussion

In very recent years, there is an increasing amount of evidence that during some last stages of the long term process of preparation, there could be a transfer of energy between lithosphere and the above layers of atmosphere and ionosphere, so as to introduce the concept of a lithosphere–atmosphere–ionosphere coupling (LAIC) among the three involved layers of the Earth system (Pulinets et al., 2000; Hayakawa and Molchanov, 2002; Molchanov et al., 2004; Pulinets and Ouzounov, 2011). On one hand, the 'energy source' is usually thought to be beneath the Earth and related with tectonic activities in the lithosphere. On the other hand, numerous rock-pressure experiments and electromagnetic observations associated with seismic activities have already proved that a giant electrical current and an abrupt increase of electromagnetic signals are motivated when the main rupture occurs for stressed-rocks. These phenomena happed on May 9 2008, 3 days before the Wenchuan event, which hypocenter lies in mid-crust. The strong seismo-telluric current is thought to run mainly along the Longmenshan fault and electromagnetic oscillations, induced by the current and predominated by ULF frequency band, propagate up to ionosphere and give rise to perturbations of ionospheric parameters. Some of these parameters have been investigated, such as GPS TEC and f0F2 (Yu et al.，2009; Xu et al., 2010; Akhoondzadeh et al., 2010), DEMETER satellite O+ density (Zhang et al., 2009), electron density and electron temperature (Zeng et al., 2009), and so on. Fortunately, all these study results present a climax on May 9 and this indicates a lithosphere–atmosphere–ionosphere coupling or interaction aroused by these electromagnetic signals prior to the Wenchuan event.

Unfortunately, at present, most of investigations put emphases on the effect of earthquakes upon the ionosphere and few of them pay attention to an inverse problem, that is the ionospheric influence on the electromagnetic waves passed through.

The ionosphere, as a part of the electrical conducting region of the upper atmosphere, can enhance electromagnetic fields and make the decay slow when an observation is within ionospheric range and the ionosperic effect can be up to 1-2 magnitudes of the electrical fields in our simply three-layer model for some specified parameters we select.

Considering the Wenchuan event, the electrical signals from the lithosphere interact with the ionosphere and are improved simultaneously, and then registered at 1440km Gaobeidian station with the amplitude of 1.3 mV m^{-1}. This electrical field is

Solid Earth Discuss., doi:10.5194/se-2016-89, 2016
Manuscript under review for journal Solid Earth
Published: 30 June 2016

used to simulate the seismo-telluric current produced by the Wenchuan main rupture in an Earth-air-ionosphere model together with an Earth-air model. The results present that, the seismo-telluric currents with and without ionospheric effect must be about 5.3×104 kA and 3.7×105 kA respectively. Compared with the expected seismo-telluric current ~10–100 kA of the "Alum Rock" M_W=5.6 earthquake for an observed 30 nT pulse at 1 Hz and D=2 km (Bortnik et al., 2010), this result is probably in a reasonable range.

However, firstly, the total rupture of the Longmenshan fault concerned with the Wenchuan main shock is extremely complicated that contains tenths rupture stages and several pauses, totaled 90 s for the whole rupture process (～300 km), according to Zhang et al.,(2009). Thus the total surface rupture ～300 km is nevertheless not used here. While performing the analysis on only the primary 30 s, a main stage of the Wenchuan earthquake, out of 90 s as we have selected L=150 km above, is expected to be representative of the majority of the rupture to generate a seismo-telluric current. Secondly, three medium are thought of as a homogeneous isotropic medium in our models and with the same average conductivity value for each one, especially for the wenchuan area. However, the Earth conductivity plays a so important role that can predominately affect the fluctuations of the electrical fields as shown in Fig.4 although no one exactly knows the right conductivity of the bottom medium. The value $\sigma_1 = 7.0 \times 10^{-4}\ \mathrm{S\ m^{-1}}$ taken part in all analysis is estimated when the observing frequency range f=0.1-10 Hz and the hypocenter depth d=19 km of the Wenchuan main event are taken into account for the skin-depth formula. One must also mention that we use f=1 Hz in our calculations because we cannot distinguish the right frequency of the recorded analog signals. All these can underscore our simulation results.

While these disadvantageous selections maybe are not so important at the same time because the key point of this paper is of ionospheric influence on electromagnetic waves and our investigation attains advantageous results.

6 Conclusions

In this paper, a three-layer (Earth-air-ionosphere) physical model, as well as a two-layer (Earth-air) model, is employed to investigate the ionospheric effect on the wave fields for a finite length dipole current source co-located with the main fault of an earthquake when an observing location distance is up to one thousand kilometers

Solid Earth Discuss., doi:10.5194/se-2016-89, 2016
Manuscript under review for journal Solid Earth
Published: 30 June 2016

or even more. For a dipole source with specified parameters of the length L=150 km, the current I=1 A, and the depth d=19 km, the results show that all fields are free of the ionospheric effect for different frequencies in relative short ranges, e.g., ~600 km for f=0.1 Hz, which implies the ionospheric influence on electromagnetic field transmissions can be neglected within this range. However, the ionosphere can strengthen the field amplitude and make the decay slow when an observation is out of this range and the ionosperic effect can be up to 1-2 magnitudes of the electrical fields.

This is suitable for the 12 May 2008 Wenchuan M_S=8.0 earthquake during which a strong electromagnetic signal with an amplitude of ~1.3 mV m^{-1}, is recorded by the Gaobeidian ULF (f=0.1-10 Hz) observing station 1440 km away from the epicenter. The main fault rupture producing a current is equivalent to a finite length dipole current source, with a nucleation depth of 19 km and a length of 150 km. Considering the Earth-air-ionosphere model, the expected current for the most typical properties of Wenchuan area is of 5.3×10^4 kA, which is of one magnitude smaller than the current value of 3.7×10^5 kA obtained with the Earth-air model free of ionospheric effect. On the contrary, a signal introduced by a seismic activity can be advantageously recorded by a remote station under the ionospheric effect as if the detectability of the system is improved effectively.

Acknowledgements and data. The authors are grateful to the National Natural Science Foundation of China and this work was sponsored by the project Simulation and Interpretation of the Spatial Electromagnetic Phenomena Coupling before the Wenchuan M_S8.0 Earthquake under grant agreement n °41204057. The data presented in this paper are available to the e-mail: limeixuxl@seis.ac.cn.

References

Akhoondzadeh, M., Parrot, M., and Saradjian M. R.: Electron and ion density variations before strong earthquakes (*M*>6.0) using DEMETER and GPS data, Nat. Hazards Earth Syst. Sci., 10, 7–18, 2010.

Bernardi, A., Fraser-Smith, A. C., McGill, P. R., and Villard Jr, O. G.: Magnetic field measurements near the epicenter of the *M*s7.1 Loma Prieta earthquake, Phys. Earth Planet, Interiors, 68, 45–63, 1991.

Bortnik, J., Bleier, T. E., Dunson, C., and Freund, F., Estimating the seismo-telluric current required for observable electromagnetic ground signals, Ann. Geophys., 28,

Solid Earth Discuss., doi:10.5194/se-2016-89, 2016
Manuscript under review for journal Solid Earth
Published: 30 June 2016

478 1615–1624, doi:10.5194/angeo-28-1615-2010, 2010.
479 Cummer, S.A.: Modeling Electromagnetic Propagation in the Earth-Ionosphere
480 Waveguide, IEEE Transactions on Antennas and Propagation, 48(9), 2–12, 2000.
481 Draganov, A. B., Inan, U. S., and Taranenko, Y. N.: ULF magnetic signatures at the
482 Earth due to groundwater flow: a possible precursor to earthquakes, Geophys. Res.
483 Lett., 18, 1127–1130, 1991.
484 Eftaxias, K., Kapiris, P., Polygiannakis, J., Peratzakis, A., Kopanas, J., Antonopoulos,
485 G., and Rigas D.: Experience of short-term earthquake precursors with VLF-VHF
486 electromagnetic emissions, Nat. Hazards Earth Syst. Sci., 3, 217–228, 2002.
487 Egbert, G. D.: On the generation of ULF magnetic variations by conductivity
488 fluctuations in a fault zone, Pure Appl. Geophys., 159, 1205–1227, 2002.
489 Fenoglio, M. A., Johnston, M. J. S., and Byerlee J. D.: Magnetic and electric fields
490 associated with changes in high pore pressure in fault zones: application to the
491 Loma Prieta ULF emissions, J. Geophys. Res., 100 (12), 951–958, 1995.
492 Fraser-Smith, A. C., Bernardi, A., McGill, P. R., Ladd, M. E., Helliwell, R. A., and
493 Villard Jr, O. G.: Low-frequency magnetic measurements near the epicenter of the
494 *M*s 7.1 Loma Prieta earthquake, Geophys. Res. Lett., 17, 1465–1468, 1990.
495 Freund, F., and Sornette, D.: Electro-magnetic earthquake bursts and critical rupture
496 of peroxy bond networks in rocks, Tectonophysics, 431, 33–47, 2007.
497 Freund, F.: Charge generation and propagation in igneous rocks, J. Geodynamics, 33,
498 543–570, 2002.
499 Freund, F.: Stress-activated positive hole charge carriers in rocks and the generation
500 of pre-earthquake signals, in: Electromagnetic Phenomena Associated with
501 Earthquakes, edited by: Hayakawa, M., Transworld Research Network, Trivandrum,
502 India, Chapter 3, 41–96, 2009.
503 Freund, F.: Toward a unified solid state theory for pre-earthquake signals, Acta
504 Geophys., 58(5), 719–766, 2010.
505 Fu, C. M., Di, Q. Y., Xu, C., and Wang, M. Y.: Electromagnetic fields for different
506 type sources with effect of the ionosphere, Chinese J. Geophys., 55(12), 3958–3968,
507 doi: 10. 6038/ j. issn. 0001-5733. 2012. 12. 008, 2012(in Chinese with English
508 abstract).
509 Guan, H. P., Han, F.Y., Xiao, W. J., and Chen, Z.Y.: ULF electromagnetic
510 observation and data processing methods, Earthquake, 23(2), 5–93, 2003(in
511 Chinese with English abstract).
512 Hao, J. Q., Qian, S. Q., Zhou, J. G., and Zhu, T.: ULF electric and magnetic
513 anomalies accompanying the cracking of rock sample, Acta Seismologica sinica,
514 25(1), 102–111, 2003 (in Chinese with English abstract).
515 Hayakawa, M., and Molchanov, O. A. (Eds.): Seismo-Electromagnetics:

Solid Earth Discuss., doi:10.5194/se-2016-89, 2016
Manuscript under review for journal Solid Earth
Published: 30 June 2016

Lithosphere-Atmosphere-Ionosphere Coupling, p. 477. Tokyo, Japan: TERRAPUB ,2002.

Key, K.: 1D inversion of multicomponent, multi-frequency marine CSEM data: Methodology and synthetic studies for resolving thin resistive layers, Geophysics, 74(2), F9–F20, 2009.

Kopytenko, Y. A., Matiashvili, T. G., Voronov, P. M., Kopytenko, E. A., and Molchanov, O. A.: Detection of ultra-low frequency emissions connected with the Spitak earthquake and its aftershock activity, based on geomagnetic pulsations data at Dusheti and Vardzia observatories, Phys. Earth Planet. Interiors, 77, 85–95, 1993.

Kuo, C. L., Huba, J. D., Joyce, G., and Lee, L. C.: Ionosphere plasma bubbles and density variations induced by pre-earthquake rock current and associated surface charges, J. Geophys. Res., 116(10), A10317, doi:10.1029/2011JA016628, 2011.

Li, M., Lu, J., Parrot, M., Tan, H., and Zhang, X.: Review of unprecedented ULF electromagnetic anomalous emissions possibly related to the Wenchuan M_S = 8.0 earthquake，on 12 May 2008． Nat． Hazards Earth Syst． Sci．, 13(2), 279–286, doi: 10. 5194/nhess-13-279-2013, 2013.

Li, D., Di, Q. Y., and Wang, M. Y.: One-dimensional electromagnetic fields forward modeling for “earth–ionosphere” mode. Chinese J. Geophys., 54(9), 2375–2388, doi: 10. 3969/ j. issn. 0001–5733. 2011. 09. 021, 2011 (in Chinese with English abstract).

Li, Y., Lin, P. R., Zheng, C. J., Shi, F. S., Xu, B. L., and Guo, P.: The electromagnetic response modeling of the ELF method and the influence of the ionosphere, Geophysical & Geochemical Exploration, 34(3), 332–339, 2010a, (in Chinese with English abstract).

Li, D. Q., Di, Q. Y., and Wang, M. Y.: Study of large scale large power control source electromagnetic with “Earth–ionosphere” mode, Chinese J. Geophys., 53(2), 411–420, doi: 10. 3969/ j. issn. 0001-5733. 2010. 02. 019, 2010b, (in Chinese with English abstract).

Molchanov, O. A., Kopytenko, Y. A., Voronov, P. M., Kopytenko, E. A., Matiashvili, T. G., Fraser-Smith, A. C., and Bernardi, A.: Results of ULF Magnetic field measurements near the epicenters of the Spitak (*M*s 6.9) and Loma Prieta (*M*s7.1) earthquakes: comparative analysis, Geophys. Res. Lett., 19, 1495–1498, 1992.

Molchanov, O. A., Fedorov, E., Schekotov, A., Gordeev, E. , Chebrov , V., Surkov, V., …, Biagi, P. F.: Lithosphere-atmosphere-ionosphere coupling as governing mechanism for preseismic short-term events in atmosphere and ionosphere, Natural Hazards Earth Syst. Sci., 4, 757-767, 2004.

Panfilov, A. A.: The results of experimental studies of VLF–ULF electromagnetic

Solid Earth Discuss., doi:10.5194/se-2016-89, 2016
Manuscript under review for journal Solid Earth
Published: 30 June 2016

554 emission by rock samples due to mechanical action, Nat. Hazards Earth Syst. Sci.,
555 14, 1383–1389, doi:10.5194/nhess-14-1383-2014, 2014.
556 Park, S. K.: Precursors to earthquakes: seismo-electromagnetic signals, Surv.
557 Geophys., 17, 493–516,1996.
558 Pulinets, S. A., and Ouzounov, D.: Lithosphere-Atmosphere-Ionosphere Coupling
559 (LAIC) model-An unified concept for earthquake precursors validation, J.
560 Southeast Asian Earth Sci., 41(4–5): 371–382, 2011.
561 Pulinets, S. A., Boyarchuk , K. A., Hegai, V. V., Kim, V. P., and Lomonosov, A. M.:
562 Quasielectrostatical model of atmosphere-thermosphere-ionosphere coupling, Adv.
563 Space Res., 26, 1209-1218, 2000.
564 Qian, S. Q., Ren, K. X., and L ü, Z.:Experimental study on VLF, MF, HF and VHF
565 electromagnetic radiation characteristics with the rock breaking, Earthquake
566 Science, 18(3), 346–351,1996 (in Chinese with English abstract).
567 Qian, S. Q., Hao, J. Q., Zhou, J. G., and Gao, J. T.:Precursory Electric and Magnetic
568 Signals at ULF and LF Bands during the Fracture of Rocks under Pressure.
569 Earthquake Research in China, 19(2), 109–116, 2003(in Chinese with English
570 abstract).
571 Sarlis, N., Lazaridou, M., Kapiris, P., and Varotsos, P.: Numerical model of the
572 selectivity effect and the V/L criterion, Geophys. Res. Lett., 26, 3245–3248, 1999.
573 Simpson, J. J., and Taflove, A.: Electrokinetic effect of the Loma Prieta earthquake
574 calculated by an entire-Earth FDTD solution of Maxwell's equations. Geophys. Res.
575 Lett., 32, L09302, doi: 10. 1029/2005GL022601, 2005.
576 Varotsos, P., and Lazaridou, M.: Latest aspects of earthquake prediction in Greece
577 based on seismic electric signals. Tectonophysics, 188, 321–347,1991.
578 Varotsos, P., Sarlis, N., and Lazaridou, M.: Transmission of stress induced electric
579 signals in dielectric media, Part II, Acta Geophys, 48, 141–177, 2000.
580 Varotsos, P., Sarlis, N., Skordas, E., Tanaka, H., and Lazaridou, M.: Additional
581 evidence on some relationship between seismic electric signals and earthquake
582 source parameters, Acta Geophys., 53, 293–298, 2005.
583 Wait, J. R.: Geo-electromagnetism: Academic Press,1982.
584 Wait, J. R.: Some Factors Concerning Electromagnetic Wave Propagation in the
585 Earth's Crust, Proc. IEEE, 54(8), August 1966.
586 Xu, C., Di, Q. Y., Fu, C. M. and Wang, M. Y.: The contrast of response
587 characteristics between large power long dipole and circle source, Chinese J.
588 Geophys, 55(6), 2097–2104, doi: 10. 6038/ j. issn. 0001–5733. 2012. 06. 03, 2012,
589 (in Chinese with English abstract).
590 Xu, T., Hu, Y., Wu, J., Wu, Z., Suo, Y., and Feng, J.: Giant disturbance in the
591 ionospheric F2 region prior to the *M*8.0 Wenchuan earthquake on 12 May 2008,

Solid Earth Discuss., doi:10.5194/se-2016-89, 2016
Manuscript under review for journal Solid Earth
Published: 30 June 2016

592 Ann. Geophys., 28, 1533–1538, 2010.
593 Xu, X. W.:Album of 5.12 Wenchuan 8.0 earthquake surface ruptures. Seismological
594 press, 2009 (in Chinese with English abstract).
595 Yamauchi, T., Maekawa, S., Horie, T., Hayakawa, M., and Soloviev, O.:
596 Subionospheric VLF/LF monitoring of ionospheric perturbations for the 2004
597 Mid-Niigata earthquake and their structure and dynamics, J. Atmos. Sol. Terr.
598 Phys., 69, 793–802, 2007.
599 Yu, T., Mao, T., Wang, Y. G., and Wang, J. S.: Study of the ionospheric anomaly
600 before the Wenchuan earthquake, Chinese Science Bulletin, 54(6): 1086–1092, doi:
601 10.1007/s11434-008-0587-8, 2009 (in Chinese with English abstract).
602 Zeng, Z. C., Zhang, B., Fang, G. Y., Wang, D. F., and Yin, H. J.: The analysis of
603 ionospheric variations before Wenchuan earthquake with DEMETER data, Chinese
604 J. Geophys., 52(1): 11–19, 2009 (in Chinese with English abstract).
605 Zhang, X., Shen, X., Liu, J., Ouyang, X., Qian, J., and Zhao, S.: Analysis of
606 ionospheric plasma perturbations before Wenchuan earthquake. Nat. Hazards Earth
607 Syst. Sci., 9: 1259–1266, 2009.
608 Zhang ,Y., Feng, W. P., Xu, L. S., Zhou, C. H., and Chen, Y. T.: Spatio-temporal
609 rupture process of the 2008 great Wenchuan earthquake, Science in China Series D:
610 Earth Sciences, 52 (2), 145–154, 2009.
611 Zhu, Y. T., Wang, X. B., Yu, N., Gao, S. Q., Li, K., and Shi, Y. J.: Longmenshan
612 magnetotelluric deep structure and the Wenchuan earthquake (M_S8.0), Acta
613 Geologica Sinica, 82 (12), 1769–777, 2008 (in Chinese with English abstract).
614